Published in IET Communications
Received on 5th March 2014
Revised on 12th June 2014
Accepted on 26th July 2014
doi: 10.1049/iet-com.2014.0230

ISSN 1751-8628

Adaptive handover algorithm in heterogeneous femtocellular networks based on received signal strength and signal-to-interference-plus-noise ratio prediction

Hashem Kalbkhani[1], Saleh Yousefi[2], Mahrokh G. Shayesteh[1,3]

[1]*Department of Electrical Engineering, Urmia University, Urmia, Iran*
[2]*Department of Computer Engineering, Urmia University, Urmia, Iran*
[3]*Wireless Research Laboratory, Electrical Engineering Department, ACRI, Sharif University of Technology, Tehran, Iran*
E-mail: m.shayesteh@urmia.ac.ir

Abstract: In this study, an efficient handover algorithm based on the received signal strength (RSS) prediction is presented for two-tier macro–femtocell networks in which, because of the fading effects of channel and short coverage range of femtocells, ping-pong handovers may take place. In the proposed approach, first each mobile station (MS) uses the recursive least square algorithm for predicting the RSS from the candidate base stations (BSs) including both femtocell and macrocell BSs. Then, according to the predicted RSS values, several future values of signal-to-interference plus noise ratio (SINR) are calculated. Afterwards, the candidate list of BSs is pruned according to the estimated future SINR values and the predicted RSS of each BS. Finally, the target BS which yields the highest throughput, is opted for handover. Through extensive simulations, the effects of speed of MSs and the density of femtocell BSs on the outage probability (OP), throughput and the ping-pong rate of MSs are studied. The results show that the proposed handover algorithm outperforms the previous ones and improves the throughput of MS while it reduces the OP and the number of ping-pong handovers.

1 Introduction

Femtocells are low power and short range cellular access points that are proposed to improve the coverage for indoor environments [1]. Owing to the small distance between users and femtocell base station (FBS), this type of access to the cellular network can provide a better signal quality for indoor users and results in a higher throughput and spectrum efficiency.

It is estimated that nearly 23% of voice calls and over 90% of data services occur in indoor environments [2]. These statistics imply that the deployments of femtocells are rapidly increasing in the future. Therefore, we may face with a large number of FBSs co-deployed in the coverage of a macrocell. Owing to mobility of mobile station (MS) nodes, by increasing the number of FBSs, the number of handovers (NHO) is increased as well. Owing to the variations of the received signal strength (RSS) and the small radius of femtocells, several unnecessary handovers may take place that increase the number of ping-pong handovers. By ping-pong, we mean the NHO in a specific time duration exceeding a threshold (e.g. more than one handover in every 5s). The ping-pong effect causes some defections including throughput reduction, long handover delay and high dropping probability, which all deteriorate the quality of service (QoS) [3]. Most of the current techniques that are based on current RSS, utilise the hysteresis margin for making handover decision aiming at reducing the ping-pong effect. It is shown that taking advantage of RSS prediction leads to better prevention of frequent handovers [4] and handover latency reduction [5].

Owing to the presence of many cellular access points with different transmission powers and coverage radiuses, traditional handover algorithms for homogeneous networks, cannot be used in macro/femtocell heterogeneous networks. In traditional handover approaches, the base station (BS) having the maximum RSS in the current time, is selected as the target BS for handover. However, channel conditions are varying continuously and there is no guarantee that the selected BS remains the best BS for a reasonably time period and thus more handovers may take place leading to the ping-pong effect. This effect is intensified by short radius of femtocells implying that we may be faced with frequent handovers with short life times. Introducing efficient handover algorithm for femtocellular environments has attracted many researchers' attention.

To overcome the asymmetry in transmission powers of FBSs and macrocell BS (MBS), an algorithm has been proposed in [6] that makes handover decisions based on the RSS of both FBS and MBS. In that mechanism, the RSS of MBS is compared with the a weighted sum of the RSS of FBS and that of MBS with the weight α. The results show

that this approach improves the probability of connection to FBS in areas near to MBS and also MSs can use better signal quality received from FBS. However, this algorithm needs the exact knowledge of FBS location to select the proper value of α. In [7], the authors proposed an algorithm based on the RSS and wireless transmission loss named RWTL in which, handover is triggered when the RSS from FBS is greater than a threshold. In fact, when the received RSS from FBS exceeds the RSS from MBS, plus a hysteresis margin, the MS connects to the FBS, otherwise transmission loss is used as handover parameter and MS connects to the BS with a minimum transmission loss. It should be noted that knowledge of the transmission powers of BSs is necessary for transmission loss calculation. It was shown that the algorithm in [7] outperforms that of [6] in terms of the probability of assignment of users to FBS. However, if the RSS of the FBS is lower than that of the MBS, making connection to the FBS results in a lower RSS which leads to throughput degradation. Another concern about the works of [6, 7] is that the performance of the methods is evaluated for nodes moving in a straight line and scenarios with dense femtocells and nodes with random mobility are not considered. Yidan *et al.* [8] proposed a mechanism for femtocell-to-femtocell handover. The candidate FBSs are selected based on their RSSs and access mode while the hidden FBS problem is taken into account as well. It was shown that the method proposed in [8] has a lower failure rate than the traditional handover algorithms.

Recently, a few works made efforts to reduce the number of unnecessary handovers in macro/femtocell networks. In [9], a cell selection method for an open-access femtocell network was modelled as a decentralised restless multi-armed bandit with unknown dynamics and multiple players. In this framework, each channel is modelled as an arbitrary finite-state Markov chain while each user tries to find the best channel that maximises its capacity and reduces the NHO. In [10], self-optimising algorithm uses kernel methods and neural networks to reduce the unnecessary handovers in a indoor–outdoor scenario. However, in such approaches the computational complexity is a main concern. A cell association algorithm with the objective of reaching a trade-off between network capacity and fairness was proposed in [11]. The algorithm reduces unnecessary handovers using Bayesian estimation and maximises network capacity while trying to maintain fairness among users. A distance-based handover scheme was proposed in [12]. In this algorithm, at first mobile user obtains the traversed distance in femtocell coverage area, and then the distance is compared with a threshold value to make a decision for handover.

A few predictive algorithms have been presented in particular for dense femtocell deployments. In [5], the authors proposed a prediction-based approach to increase service continuity, which in turn leads to reduction of handover latency. Autoregressive (AR) model for prediction of the filtered reference signal received power of Layer 3 (L3) is used to activate L3 handover prior to Layer 2 (L2) handover procedure. Their method at first triggers the classical handover (i.e. based on the current RSS) and if handover is not triggered, the predictive approach is used to trigger the handover in L3. In [13], the authors introduced an algorithm that predicts the future mobility pattern of MSs to identify temporary femtocell visitors to reduce the unnecessary handovers. The location of the MS is determined by a positioning technology and is sent to the server periodically. The server extracts mobility patterns, and if the next movements are located in the femtocell coverage area for a long enough time, the MS connects to the FBS.

The aim of this study is to present an efficient handover algorithm in order to improve the throughput of MSs and reduce the ping-pong handovers. Our approach is a prediction-based algorithm and is different from the previous prediction-based approaches [4, 5, 13]. In the proposed method, we utilise RSS in order to trigger handovers. At first, the BSs whose related RSS are greater than a threshold and also greater than the RSS of the serving BS plus a hysteresis margin, are identified. Then, we predict the future RSS samples of the identified BSs (obtained in the previous step) and the current serving BS. Adaptive recursive least square (RLS) algorithm [14] is used to predict the RSS samples which are used for estimation of the future SINR samples. Finally, we prune the list of candidate BSs based on the estimated SINR and predicted RSS and choose the BS with the highest throughput. The performance of the proposed algorithm is evaluated in terms of error in RSS prediction, the NHO, the ping-pong rate (PPR), the throughput and outage probability (OP) of the MSs. The results indicate the efficiency of the introduced algorithm in comparison with previous methods.

The rest of this paper is organised as follows. Section 2 describes the two-tier cellular network model used in this work. Description of the RLS algorithm and prediction details are presented in Section 3. The proposed neighbour BSs list creation and handover algorithm are explained in Section 4. Performance evaluation results are provided in Section 5. Finally, Section 6 concludes the paper.

2 Network model

We consider downlink of the orthogonal frequency-division multiple access-based two-tier cellular network. The macrocell network layout and spectrum partitioning are shown in Figs. 1*a* and *b*, respectively. The central macrocell is surrounded by 6 and 12 macrocells in the first and second layers of the macrocell network, respectively. Therefore, a macrocell network consists a total of 19 macrocells. Since the distance of higher layers (layers three and later) of the macrocell network from the central macrocell is large, the received interferences from them is negligible; hence the effect of higher tier macrocells is ignored.

In this paper, we consider the coverage area of the central macrocell. Macrocell network follows fractional frequency reuse structure, where the coverage area is divided into two non-overlapping regions; inner and outer regions. The radius of inner region is selected in a manner that both regions have the same areas. An omni-directional antenna is used at the centre of the hexagonal macrocell with radius R_m to serve macrocell users with different transmission powers for the inner and outer regions users [15, 16].

We adopt frequency partitioning and an allocation scheme presented in [17]. Frequency spectrum (20 MHz) is divided into four sub-bands, namely F_a, F_b, F_c and F_d, to provide 100 resource blocks (RBs) each with 200 kHz bandwidth. F_a is allocated to the macrocell users in the inner area with a frequency reuse factor equal to one. The remaining sub-bands are assigned to the macrocell users in the outer area with frequency reuse factor equal to three. From the available sub-bands, femtocell network uses RBs from the

doi: 10.1049/iet-com.2014.0230

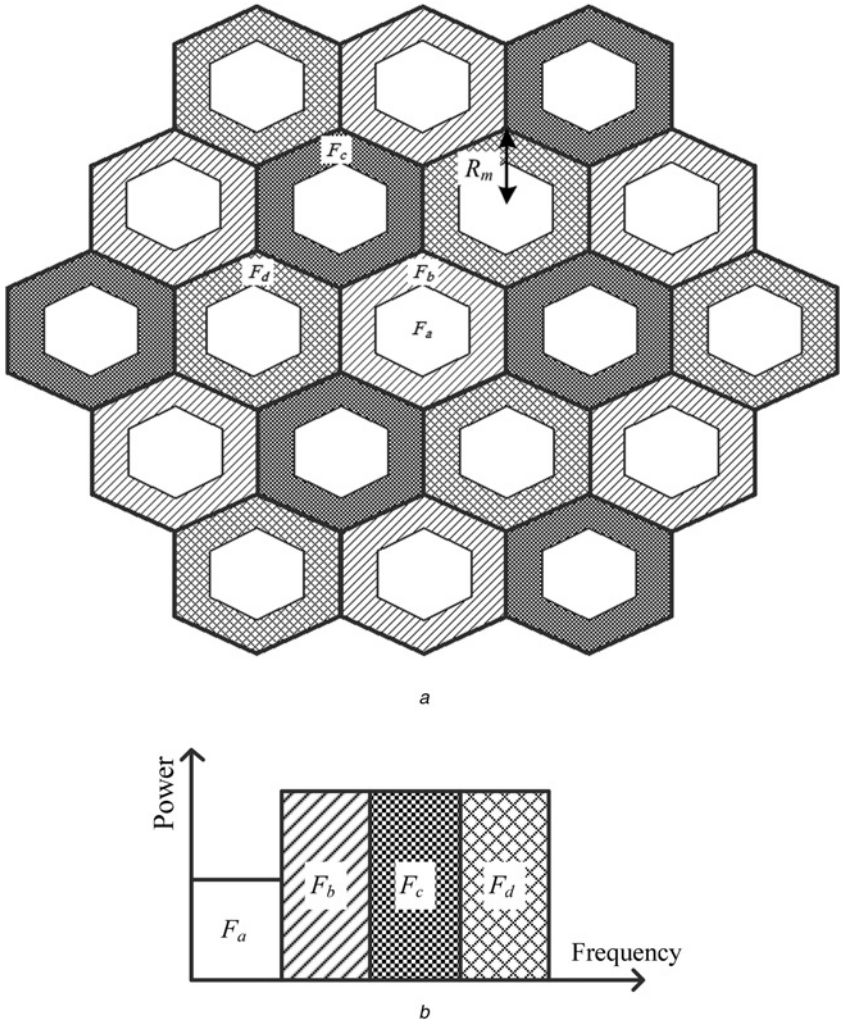

Fig. 1 *Macrocell network layout and frequency partitioning used in this study*

a Macrocell network layout
b Spectrum division

sub-bands F_c and F_d to avoid high cross-tier interference from the macrocell network in co-channels. In this study, it is assumed that femtocell network can use eight RBs with lowest cross-tier interference from sub-bands F_c and F_d. Each FBS randomly chooses one RB to serve its user with an omni-directional antenna. FBSs are distributed in the coverage area of macrocell according to the homogeneous spatial Poisson point process with intensity λ_F to coverage the disk area with radius R_F. Therefore, the average number of FBSs in the cover of the central macrocell with area $|\mathcal{H}|$ is $N_{\text{FBS}} = \lambda_{\text{F}}|\mathcal{H}|$.

Path loss, shadowing and frequency-flat Rayleigh fading are considered to model the wireless channel. Path losses of different links are presented in Table 1, which are adopted from [18]. In Table 1, d denotes the distance between the transmitter and receiver, L_{w} is the wall penetration loss and d_{indoor} is the nearest available distance from FBS to MS that is set to 0.5 m.

Shadowing has log-normal distribution, that is, its logarithm has normal distribution with mean μ and standard deviation σ [19]. It is assumed that shadowing fluctuations have the correlation distance equal to d_0; shadowing coefficients have autocorrelation function as

$$r_k = \sigma^2 \mathrm{e}^{-k/d_0} \tag{1}$$

Table 1 Path losses for different links [18]

Link (Tx/Rx)	Path loss
MBS/outdoor user	$P_{\text{L}}(\text{dB}) = 15.3 + 37.6 \log_{10} d$
MBS/indoor user	$P_{\text{L}}(\text{dB}) = 15.3 + 37.6 \log_{10} d + L_{\text{w}}$
serving FBS/indoor user	$P_{\text{L}}(\text{dB}) = 38.46 + 20 \log_{10} d + 0.7 d_{\text{indoor}}$
interfering FBS/outdoor user	$P_{\text{L}}(\text{dB}) = 38.46 + 20 \log_{10} d + 0.7 d_{\text{indoor}} + L_{\text{w}}$
interfering FBS/indoor user	$P_{\text{L}}(\text{dB}) = 38.46 + 20 \log_{10} d + 0.7 d_{\text{indoor}} + \begin{cases} L_{\text{w}}, & \text{if } R_{\text{F}} < d \le 2R_{\text{F}} \\ 2L_{\text{w}}, & \text{if } 2R_{\text{F}} \le d \end{cases}$

Also, fast fading channel coefficients have unit mean exponential distribution [20].

Based on the mentioned channel impairments, the received power P_R can be calculated as

$$P_R = P_T H \Psi P_L^{-1} \tag{2}$$

where P_T, H, Ψ and P_L indicate the BS transmission power, fast fading coefficient, log-normal shadowing and path loss, respectively.

The received SINR of an RB, γ is calculated as

$$\gamma = \frac{P_R}{I_F + I_M + N_0} \tag{3}$$

where P_R is the received power from the serving BS, I_F is the received interference from the other co-channel FBSs, which is set to zero if the serving BS is MBS, I_M is the total received interference from the interfering co-channel MBSs and N_0 is the white noise power.

In this paper, three QoS parameters from the viewpoint of the user are considered: OP, throughput and PPR. The OP of an RB is defined as the probability that its SINR becomes smaller than the predefined threshold value γ^{th}, that is

$$\text{OP} = \Pr(\gamma < \gamma^{th}) \tag{4}$$

The throughput is calculated from the Shannon entropy law [21] as follows

$$r = \log_2(1 + \gamma) \text{ bits/s/Hz} \tag{5}$$

Ping-pong occurs when the NHO in a specific time duration exceeds a threshold (e.g. more than one handover in every 5s). The PPR is calculated as the number of ping-pong handovers divided by the total NHO.

3 RLS algorithm

As mentioned, our approach is based on the RSS prediction. In this section, we briefly explain the theory of RLS [14]. The details of how it is used in our proposed method will be explained in Section 4. In the literature, adaptive prediction algorithms are used in many scenarios such as prediction of orthogonal frequency-division multiplexing time-varying channels [22], resource estimation of video decoding [23], speech encoding [24], lossless compression of floating-point volume data and video sequence [25, 26].

To overcome the random effects of shadowing and Rayleigh fading, at the receiver, exponential smoothing window is applied to the RSS; then the smoothed RSS is used as the input of RLS algorithm. The smoothing window has the impulse response as [27]

$$h_w(k) = \frac{1}{d_{avg}} \exp\left(\frac{-k}{d_{avg}}\right) \quad k \geq 0 \tag{6}$$

where d_{avg} is the smoothing window period. The smoothed RSS $(\bar{P}_R)$ is obtained by the convolution of the raw RSS (P_R) and the smoothing window as

$$\bar{P}_R(k) = P_R(k)^* h_w(k) = \frac{1}{d_{avg}} \int_0^k P_R(k-x) \exp\left(\frac{-x}{d_{avg}}\right) \mathrm{d}x \tag{7}$$

where * denotes convolution operator.

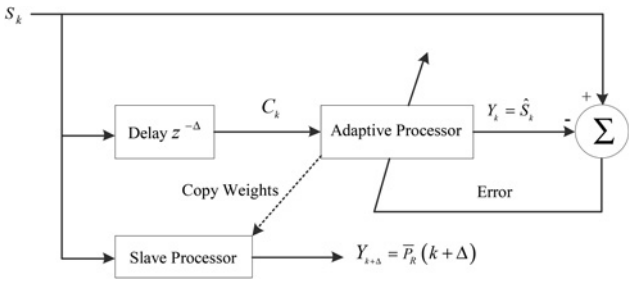

Fig. 2 *Structure of adaptive prediction [28]*

Fig. 2 illustrates the adaptive prediction block diagram [28], where the adaptive processor is a finite impulse response (FIR) filter with length F_l. Adaptive prediction consists of two steps: FIR filter coefficients estimation and then using the estimated coefficients for prediction. We denote N_{obs} as the number of RSS samples required for prediction. At first, the last N_{obs} RSS samples up to time index k, construct the signal vector S_k as

$$S_k = \left[\bar{P}_R(k - N_{obs} + 1), \quad \bar{P}_R(k - N_{obs}), \quad \ldots, \quad \bar{P}_R(k)\right] \tag{8}$$

This signal is used at the FIR filter coefficients estimation step. Then, based on the Δ delayed sample version of S_k, that is, C_k, the last Δ samples of S_k are predicted.

At the ith iteration of the estimation step, the RSS sample vector $(\boldsymbol{X}_i)$ and the weight vector $(\boldsymbol{W}_i)$ used in the adaptive processor are, respectively, defined as

$$\boldsymbol{X}_i = \left[C_k(i) C_k(i-1), \ldots, \; C_k\left(i - F_1 + 1\right)\right] \tag{9}$$

$$\boldsymbol{W}_i = \left[w(0) \quad w(1), \ldots, \; w\left(F_1 - 1\right)\right]^T \tag{10}$$

where $[.]^T$ denotes the transpose operation. The output of the adaptive processor at the ith iteration is obtained as

$$\hat{S}_k(i) = \boldsymbol{X}_i \boldsymbol{W}_i \tag{11}$$

The error, that is, the difference between the actual RSS sample and the predicted RSS one, is calculated as

$$e_k(i) = S_k(i) - \hat{S}_k(i) \tag{12}$$

The RLS algorithm tires to reduce $E\left[e_k^2(i)\right]$ and updates the weight vector at the ith iteration as [14]

$$\boldsymbol{W}_i = W_{i-1} + P_i X_i^* \left[S_k(i) - X_i W_{i-1}\right], \quad i \geq 1 \tag{13}$$

where

$$P_i = \lambda_{rls}^{-1} \left[P_{i-1} - \frac{\lambda_{rls}^{-1} P_{i-1} X_i^* X_i P_{i-1}}{1 + \lambda_{rls}^{-1} X_i P_{i-1} X_i^*}\right] \tag{14}$$

Here $0 < \lambda_{rls} \leq 1$ is the forgetting factor that accounts for

doi: 10.1049/iet-com.2014.0230

possible non-stationarity of the input. In this work, λ_{rls} is set to 0.99 [14]. The initial value P_0 is set to $\varepsilon^{-1}I_{F_1}$, where ε is a small positive scalar value, and $\boldsymbol{I}_{F_1}$ is the identity matrix of size $\boldsymbol{F}_1 \times \boldsymbol{F}_1$.

After the estimation process of filter coefficients is performed, the filter weights are copied in the slave processor to predict the future Δ sample of S_k, that is, $\hat{\bar{P}}_{\text{R}}(k+\Delta)$ as

$$\hat{\bar{P}}_{\text{R}}(k+\Delta) = \left[\bar{P}_{\text{R}}(k) \quad \bar{P}_{\text{R}}(k-1), \ldots, \bar{P}_{\text{R}}\left(k-F_1+1\right)\right]\boldsymbol{W} \tag{15}$$

where $\boldsymbol{W}$ is the weight vector obtained at the end of the estimation process.

4 Proposed handover algorithm

The flowchart of proposed algorithm for selecting target BS is shown in Fig. 3. The introduced algorithm consists of two main steps: (i) creating the neighbour candidate BSs list for handover, and (ii) selecting the proper BS for handover. In the following, each part is explained in details.

In a pre-determined time interval (one second in this study), each MS measures the RSSs from different BSs including MBS and FBSs. Therefore, the total number of BSs (N_{BS}) is equal to $N_{\text{FBS}}+1$, where N_{FBS} is the number FBSs. According to box 1 in Fig. 3, the BSs whose measured RSS values satisfy the following conditions, compose the set of candidate BSs $\left(S^1_{\text{HC}}\right)$

$$\bar{P}^j_{\text{R}} > P^{\text{th}}_{\text{R}} \quad \text{and} \quad \bar{P}^j_{\text{R}} > \bar{P}^{\text{serv}}_{\text{R}} + \Delta_{\text{H}} \quad \underset{j \neq \text{serving BS}}{j = 1{:}N_{\text{BS}}} \tag{16}$$

where $\bar{P}^j_{\text{R}}$, P^{th}_{R} and $\bar{P}^{\text{serv}}_{\text{R}}$ are the RSS of the jth BS, the threshold value for the RSS and the RSS of current serving BS, respectively, and Δ_{H} is the hysteresis margin. P^{th}_{R} is to make sure about the acceptable RSS from BS. If no BS belongs to S^1_{HC}, handover is not required; otherwise the next steps of the proposed algorithm are executed.

To overcome the shortcomings of classic non-predictive RSS-based handover algorithms (e.g. those of [6, 7]), we propose to predict the RSS and SINR samples of the candidate BSs that belong to S^1_{HC}. As shown in box 2 of Fig. 3, based on the N_{obs} RSS samples of the jth BS belonging to S^1_{HC}, we predict the N_{pr} RSS samples of that BS based on the RLS algorithm explained in Section 3. Thus, each MS has the predicted RSS for all BSs belonging to its S^1_{HC} list, where the predicted RSS samples of the jth BS belonging to S^1_{HC} are denoted by $\hat{\bar{P}}^j_{\text{R}}$.

Next, according to the predicted RSS samples, we estimate the next SINR samples as follows (box 3 in Fig. 3). If the user connects to the macrocell network, it receives interference only from other macrocells, while if it connects to the femtocell network, it receives interference from macrocells as well as femtocells. Since users move in a low speed (maximum 3.3 m/s), distance variations between the user and interfering macrocells are very low, therefore the variations of interference from macrocell network are negligible. To decrease the computational cost, we can assume that the received interference from the macrocell network in the next steps is the same as the interference in the current one. On the other hand, the distance between FBSs is low, hence, the received interference from other femtocells can change considerably even in very low speeds. Each femtocell user receives interference from some co-channel FBSs in the coverage of central macrocell. To estimate the received interference from other co-channel

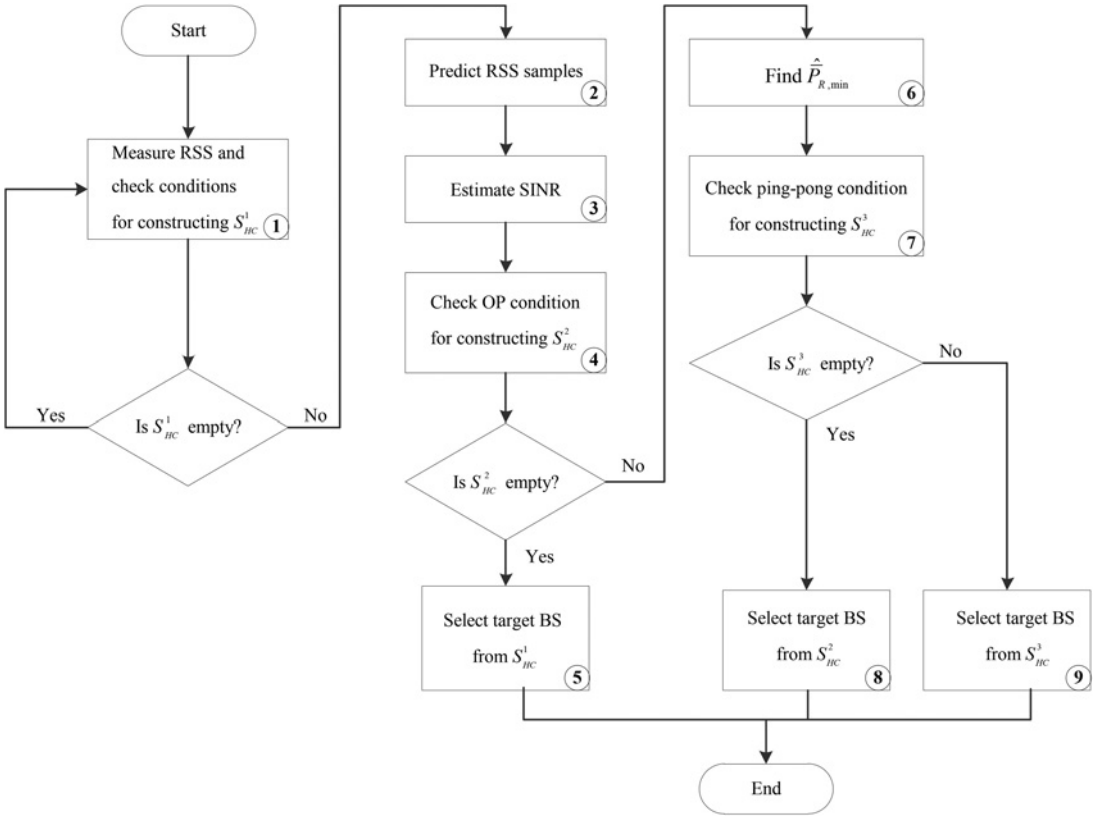

Fig. 3 *Flowchart of the proposed algorithm for selecting the target BS*

FBSs, we use the estimated interference from the co-channel interfering FBSs in S_{HC}^1. Thus, the predicted SINR of MS from the jth BS belonging to the S_{HC}^1, $\hat{\gamma}_j$ can be calculated as

$$\hat{\gamma}_j = \frac{\hat{\hat{P}}_{\mathrm{R}}^j}{I_M^j + \hat{I}_F^j + N_0} \tag{17}$$

where $\hat{\hat{P}}_{\mathrm{R}}^j$ is the predicted RSS of the jth BS, $\hat{I}_F^j$ is the predicted received interference of the jth BS from co-channel FBSs which is set to zero if the jth BS is MBS, and I_M^j is the received interference from the co-channel macrocells at the current time. As mentioned above, the received interference from co-channel MBSs is not predicted and assumed to be fixed during prediction process because of large distance between the MS and interfering macrocells and the low speed of MS.

Those BSs from S_{HC}^1 whose minimum predicted SINR values are greater than the predefined threshold value γ^{th} compose S_{HC}^2 (box 4 in Fig. 3). If all members of S_{HC}^1 have minimum predicted SINR values less than γ^{th}, S_{HC}^2 has no member. In this case (see box 5 in Fig. 3), the throughputs of candidate BSs belonging to S_{HC}^1 are estimated based on the predicted SINR values. The BS that has the maximum estimated throughput is selected as the target BS for handover. Therefore, for the jth BS of S_{HC}^1, we calculate the sum of the predicted SINR samples, that is, $S_1(j)$ as

$$S_1(j) = \sum_{n=1}^{N_{\mathrm{pr}}} \hat{\gamma}_j(n) \quad j = 1, \ldots, N_1 \tag{18}$$

where $\hat{\gamma}_j(n)$ denotes the nth predicted SINR sample of the jth BS, N_{pr} is the number of predicted RSS/or SINR samples and N_1 is the number of BSs belonging to S_{HC}^1. Finally, the target BS for the next time is obtained as

$$j_{\mathrm{target}} = \arg \max_{j \in S_{\mathrm{HC}}^1} \left(S_1(j)\right) \tag{19}$$

In the case that S_{HC}^2 has members, we check the ping-pong constraint on the BSs of S_{HC}^2 (boxes 6 and 7 in Fig. 3). Ping-pong occurs when more than one handover occurs at the specific time. In this paper, it is assumed ping-pong occurs when the MS connects to the BS for less than 5 s. The minimum value of predicted RSS samples is calculated (box 6 in Fig. 3), that is

$$\hat{\hat{P}}_{\mathrm{R,\,min}}^j = \min\left(\left[\hat{\hat{P}}_{\mathrm{R}}^j(1), \ \ldots, \ \hat{\hat{P}}_{\mathrm{R}}^j(N_{\mathrm{pr}})\right]\right) \tag{20}$$

Those BSs of S_{HC}^2 whose minimum predicted RSSs are greater than the $P_{\mathrm{R}}^{\mathrm{th}}$, construct the S_{HC}^3 (box 7 in Fig. 3). This is to make sure that the candidate BSs with the acceptable predicted SINRs can provide acceptable RSSs in the next times.

If S_{HC}^3 is an empty set, the proper BS for handover should be selected from S_{HC}^2 (box 8 in Fig. 3). The sum of the predicted SINR samples of the jth BSs of S_{HC}^2 ($S_2(j)$) is calculated as

$$S_2(j) = \sum_{n=1}^{N_{\mathrm{pr}}} \hat{\gamma}_j(n) \quad j = 1, \ldots, N_2 \tag{21}$$

where N_2 is the number of BSs belonging to S_{HC}^2. In this case, the target BS for the next time is selected as

$$j_{\mathrm{target}} = \arg \max_{j \in S_{\mathrm{HC}}^2} \left(S_2(j)\right) \tag{22}$$

If S_{HC}^3 is not empty (box 9 in Fig. 3), the sum of predicted SINRs of S_{HC}^3 is calculated as

$$S_3(j) = \sum_{n=1}^{N_{\mathrm{pr}}} \hat{\gamma}_j(n) \quad j = 1, \ \ldots, N_3 \tag{23}$$

where N_3 is the number of BSs belonging to S_{HC}^3. Finally, the BS with the maximum sum is selected as the target BS as

$$j_{\mathrm{target}} = \arg \max_{j \in S_{\mathrm{HC}}^3} \left(S_3(j)\right) \tag{24}$$

5 Performance evaluation

In this section, we evaluate the performance of the proposed handover algorithm in femtocellular networks through extensive simulations carried out in MATLAB® environment. Simulation parameters used in this work are presented in Table 2.

Among the available RBs in the sub-bands F_c and F_d, eight RBs are allocated to each FBS. Also, 100 mobile nodes are moving in the coverage area of central macrocell. Spatio-temporal parametric stepping (STEPS) mobility model [29] is used to generate the mobility pattern of users. The area of macrocell is partitioned into 20×20 grids of size 50 m × 50 m, therefore, there are 400 zones in the coverage of one macrocell.

Table 2 Simulation parameters

Parameter	Value	Parameter	Value
MBS transmission power for inner and outer area	40 and 43 dBm	standard deviation of femtocell and macrocell (σ_{F}, σ_{M})	10 and 8 dB
FBS transmission power	20 dBm	length of FIR filter in RLS (F_{l})	5
macrocell/femtocell radius ($R_{\mathrm{M}}/R_{\mathrm{F}}$)	500/20 m	number of predicted samples (N_{pr})	5
inner area radius (R_{th})	330 m	number of observation samples (N_{obs})	variable
FBS density (λ_F)	variable	RSS threshold $\left(P_{\mathrm{R}}^{\mathrm{th}}\right)$	variable
penetration loss (W_{L})	10 dB	hysteresis margin (Δ_{H})	2 dB
correlation distance (d_0)	30	mobile user speed (km/h)	2, 5, 8 and 12
smoothing filter period (d_{avg})	20	ping-pong threshold	more than one handovers in five steps
white noise power (N_0)	−174 dBm/Hz	simulation time	10^4 s

doi: 10.1049/iet-com.2014.0230

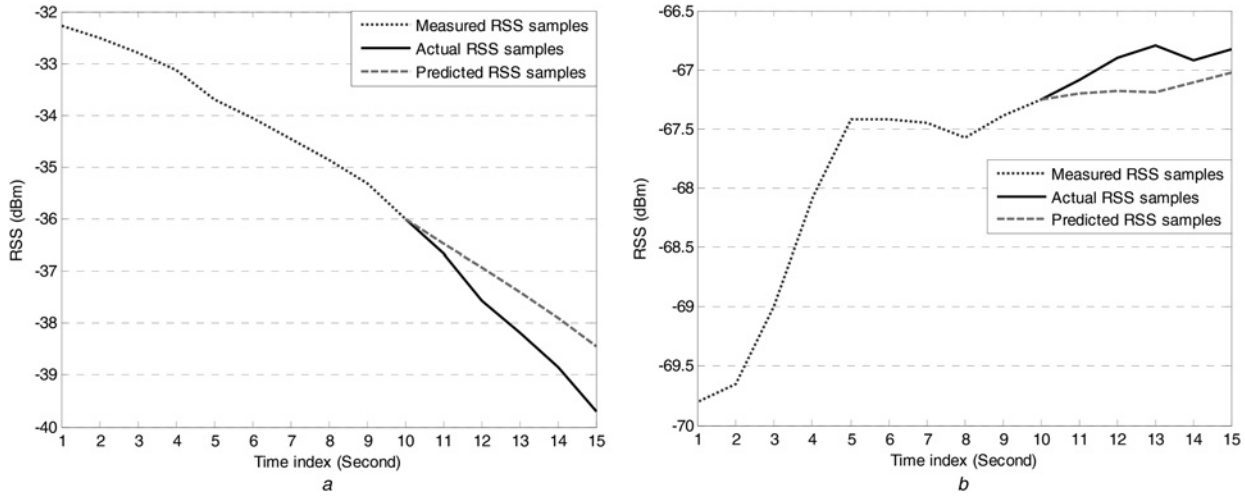

Fig. 4 *Predicted RSS samples based on previous RSS samples using the RLS-based predictor, $N_{obs} = 10$, $N_{pr} = 5$, $F_l = 5$*

a Descending scenario
b Ascending scenario

The residence time of MS in each zone is chosen randomly from uniform distribution in the range [120, 600] seconds. The maximum pause time of MSs in each way point is set to 15s. The speed of MS remains fixed during simulation time, and for each speed mentioned in Table 2, we calculate the performance of the proposed method.

The threshold for outage γ^{th} depends on the QoS requirements and it is set to 5 dB here as in [30]. Also, the ping-pong threshold is chosen according to [31], however, one can use a different value depending on his definition of ping-pong.

5.1 Performance of the RLS-based RSS prediction

In this part, we assess the performance of the proposed RLS-based prediction algorithm which is the basic element of our introduced handover approach. In Fig. 4, for both ascending and descending RSS scenarios, the predicted RSS samples based on the observed RSS samples are depicted, where an FIR filter with length five and $N_{obs} = 10$ measured RSS samples are used to predict the next five RSS samples. The coefficients of FIR filter are obtained based on the RLS algorithm, explained previously. It is observed that in both scenarios, the RLS algorithm efficiently predicts the RSS samples with high accuracy.

The performance of RLS algorithm in prediction of RSS samples is presented in terms of mean-squared-error (MSE) and mean-normalised-absolute-error (MNAE) in Figs. 5*a* and *b*, respectively. The results are obtained using all predicted RSS samples during simulation time. We observe that by increasing the number of observed samples (N_{obs}), both MSE and MNAE increase. The reason is that the non-recent samples of RSS may not represent the current status of the channel sufficiently. Therefore, it is better to limit the number of training samples (i.e. N_{obs}) to a reasonable threshold (simulations show that ten samples achieve a good prediction performance).

Also as followed from Fig. 5, for a constant N_{obs}, as the speed increases, both metrics increase. The reason is that when speed increases, because of the fast variations of the user distance from BSs, variations of RSS increase which makes the RSS prediction more complicated and consequently, the accuracy of the prediction degrades.

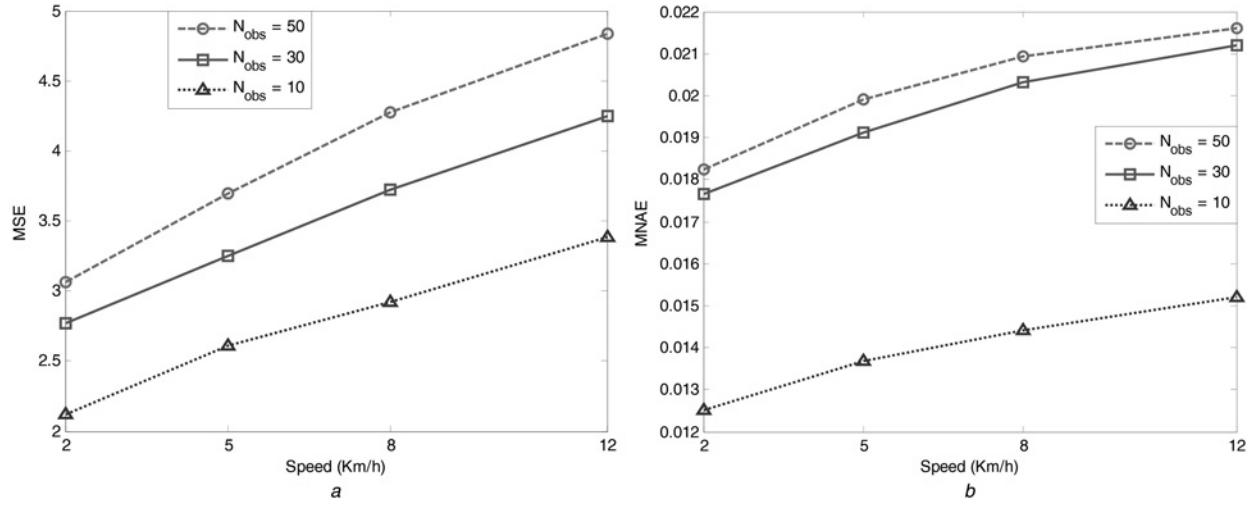

Fig. 5 *Performance of RLS-based RSS prediction algorithm in terms of*

a MSE
b MNAE

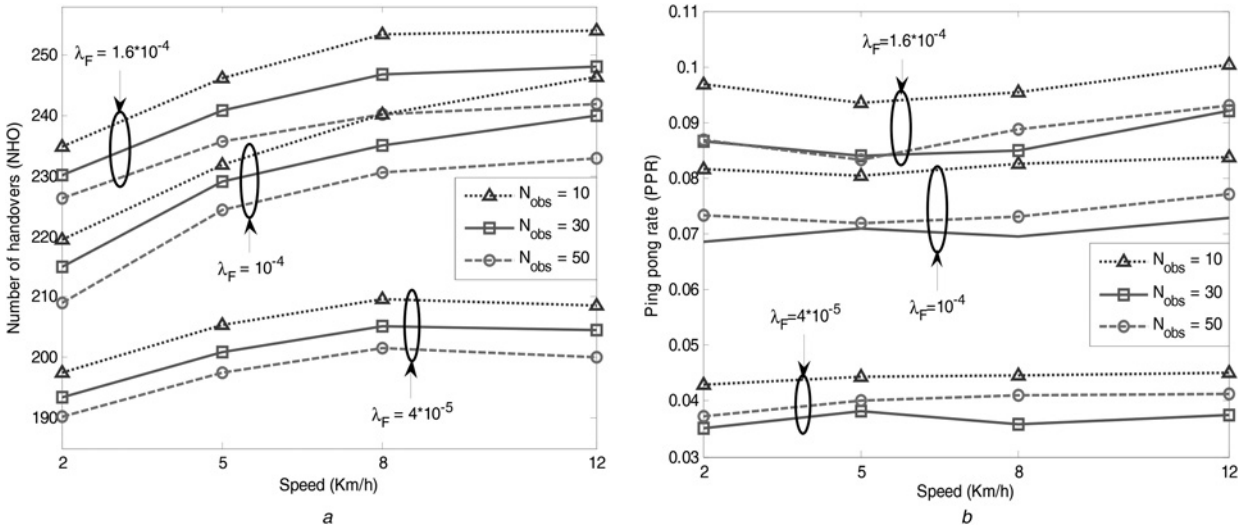

Fig. 6 *Performance of the proposed algorithm in terms of*

a NHO
b PPR

5.2 Assessing the NHO and PPR

In Fig. 6, for different FBS densities (i.e. λ_F), the average NHO and the average PPR are shown for different speeds and N_{obs}s. The PPR is defined as the ratio of ping-pong handovers to the total number of the handovers. As expected, by increasing the number of FBSs, NHO and PPR also increase for all speeds and N_{obs}. For the same N_{obs} in all densities, the increase in speed results in the increase in NHO and PPR. The reason is that, as speed increases, the residential time of MS in the coverage of FBS reduces, therefore, NHO and PPR increase. Moreover, as illustrated in the figure, when the density increases the NHO increases which in turn leads to higher PPRs.

5.3 Assessing the throughput and OP

The average throughput and OP of the proposed algorithm are shown in Fig. 7. The threshold value for acceptable SINR is set to 5 dB. It should be noted that the threshold of 5 dB for outage is chosen arbitrary and is the same in all algorithms for fair comparison. Obviously, higher values of this threshold increase the OP.

As observed, increasing the speed degrades the performance in terms of throughput and OP. For constant density of FBSs, the number of observations equal to N_{obs} = 10 achieves the best throughput and OP. Therefore, using long history in prediction of the next RSS samples does not necessarily result in high performance. Moreover,

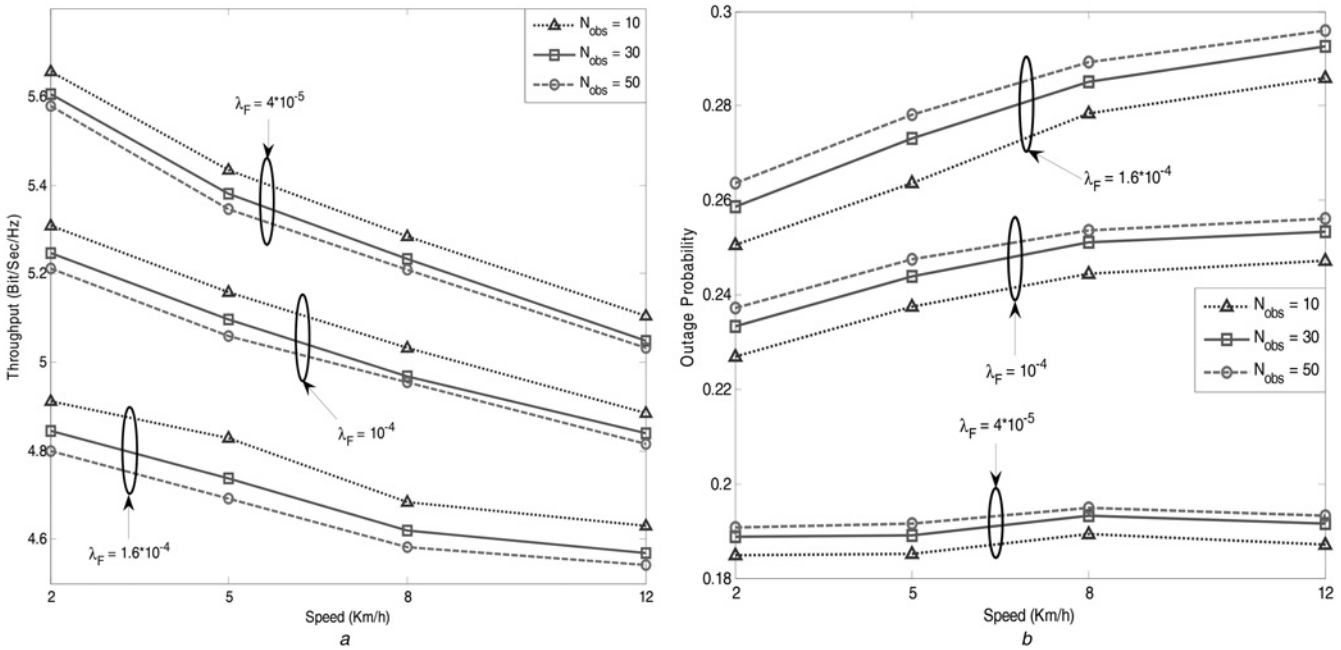

Fig. 7 *Performance of the proposed algorithm in terms of*

a Throughput
b OP

doi: 10.1049/iet-com.2014.0230

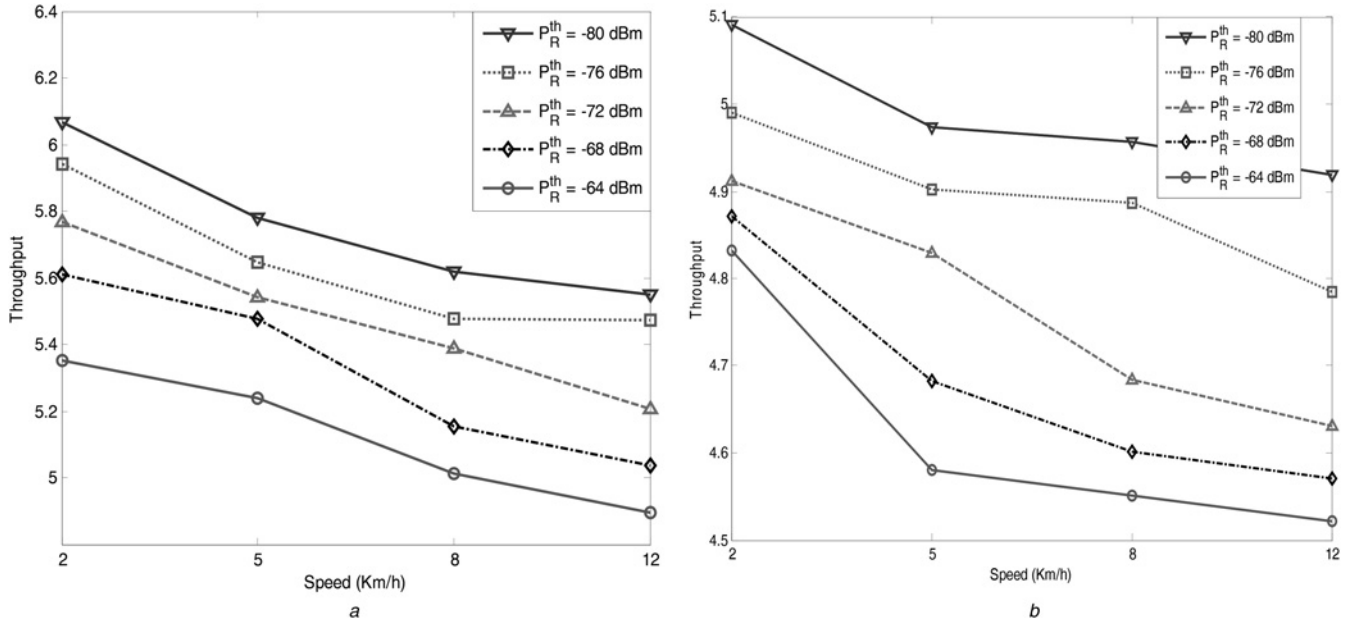

Fig. 8 *Average throughput of the proposed algorithm against the speed for different RSS threshold values and FBS densities*
a $\lambda_F = 4 \times 10^{-5}$
b $\lambda_F = 1.6 \times 10^{-4}$

increasing N_{obs} increases the computational complexity. It is seen that the proposed algorithm can perform well with low number of previous RSS samples. Also, the performance degrades as the number of FBSs increases (i.e. higher values of λ_F), which is because of the increase of interference.

5.4 Effect of RSS threshold value

According to (16), the primary neighbour list (i.e. S_{HC}^1) contains the BSs holding the following two conditions: First, their RSS values are greater than that of the serving BS; second, their RSS values are greater than the RSS threshold value (P_R^{th}). To investigate the effect of P_R^{th} on the performance of the proposed algorithm, we set up simulations with different values of P_R^{th} from -64 to -80 dBm by steps of 4 dBm. The resulted throughputs and PPRs are illustrated in Figs. 8 and 9, respectively. When P_R^{th} is high, more candidate BSs are excluded from S_{HC}^1, thus, less candidates are considered for handover. In such a situation, there might be some BSs whose RSS values are greater than that of the serving BS (and thus can offer a higher throughput). However, they are not considered for possible handover because their RSS values are less than P_R^{th}. Fig. 8 confirms this issue where lower P_R^{th} results in higher throughput. On the other hand, since lower P_R^{th} causes more unstable BSs included in S_{HC}^1, the PPR is increased as shown in Fig. 9, which is not actually desirable. In this paper, we take $P_R^{th} = -72$ dBm similar to

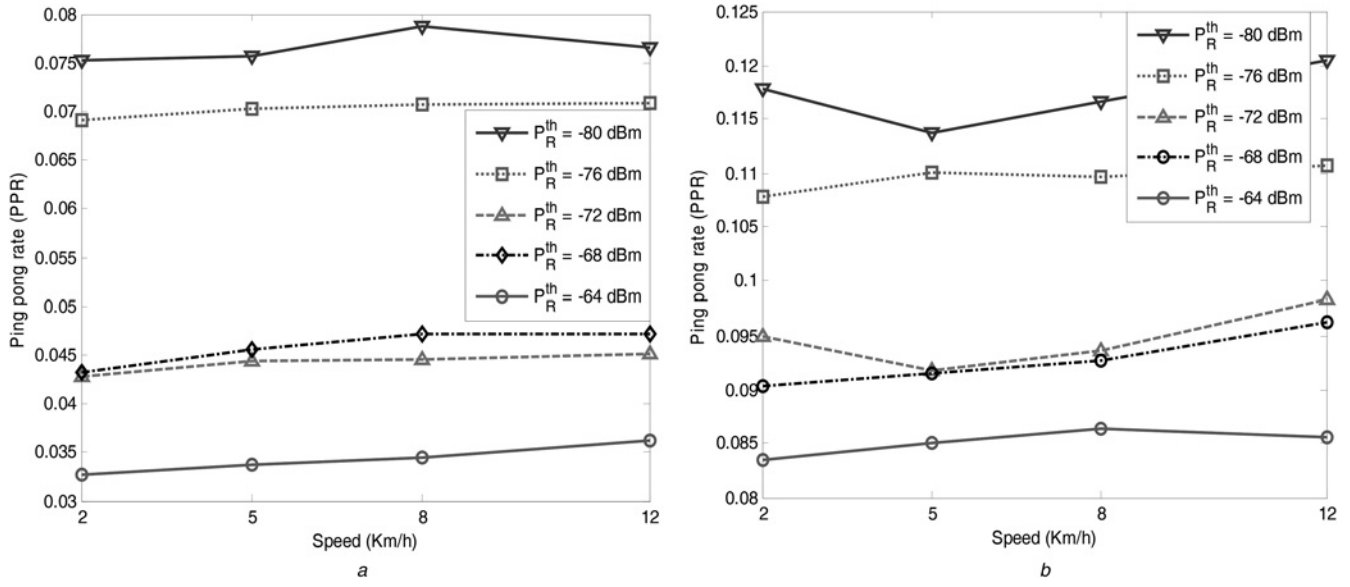

Fig. 9 *PPR of the proposed algorithm against the speed for different RSS threshold values and FBS densities*
a $\lambda_F = 4 \times 10^{-5}$
b $\lambda_F = 1.6 \times 10^{-4}$

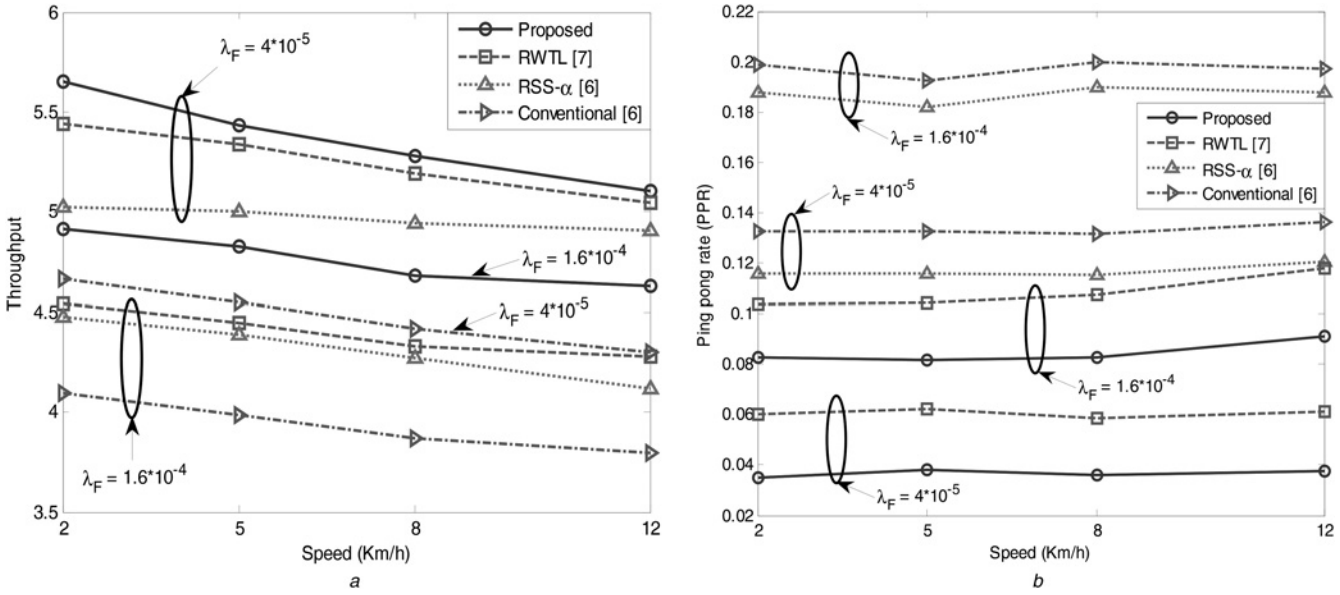

Fig. 10 *Performance comparison of the proposed method with other handover algorithms*

a Throughput
b PPR

some other works in the literature [6, 7], which provides a good trade-off between the throughput and PPR.

5.5 Comparison with the conventional handover algorithms

Finally, we compare the performance of the proposed RSS prediction-based algorithm with the conventional algorithm [6], RSS-α [6] and RTWL [7]. In the conventional algorithm, at first the neighbour list is constructed based on the current RSS samples according to (16), and then, the user connects to the BS, which has the maximum current RSS value. In the RSS-α algorithm [6], a weighted sum of the RSSs of both MBS and FBS is used to make decision to overcome the difference between the transmission powers of the MBS and the FBS, where α is used to weight the RSS of MBS. It is noted the parameter α depends on the distance of FBS from origin. It is worth mentioning that if the weighting parameter is set to zero, RSS-α algorithm behaves the same as the conventional algorithm. In RWTL algorithm [7], both RSS and wireless transmission loss are used to make decision for handover. In Fig. 10, the performance of the proposed algorithm is compared with the conventional, RSS-α, and RWTL algorithms in terms of throughput and PPR. As observed, our proposed algorithm outperforms the other three algorithms. That is, it results in a higher throughput and a lower PPR for different densities of FBSs (i.e. different values of λ_F). Furthermore, increasing λ_F degrades the performance of all algorithms, as expected.

5.6 Computational complexity

At the step of finding the target BS, our algorithm does not need any control messages to be exchanged. From the viewpoint of computational complexity, the main complexity of the proposed algorithm is in the step of predicting next RSS samples using RLS algorithm. In each iteration, RLS requires $F_l^2 + 5F_l + 1$, $F_l^2 + 3F_l$ and 1 multiplications, additions and division, respectively [14], where F_l is the length of FIR filter used for RSS prediction. Therefore, the overall complexity of the RLS algorithm is of order $O(F_l^2)$ per iteration. In [6], the main complexity is in finding the optimal value of α and in [7], in order to calculate transmission loss, the transmission powers of FBSs are needed to be known using some control messages. The imposed computational overhead of our algorithm is higher than those of [6, 7]. However, since $F_l = 5$ and the size of S_{HC}^1 is limited according to real-life FBS density, the overhead is quite tolerable for todays' technology of user equipment, such as, typical smart phones. On the other hand, according to Fig. 10, the performance of our algorithm is higher than those of the other algorithms. In particular, the lower PPR leads to decreasing handover signalling overhead, which is one of advantages of our algorithm compared to [6, 7].

6 Conclusions

In the future, it is predicted that plenty of femtocells will be deployed in the overage of current macrocells, which increase the chance of ping-pong handovers. Aiming at reducing such handovers, in this paper, an efficient handover algorithm based on the prediction of RSS and obtaining the future SINR values of the candidate BSs was proposed. We take advantage of the RLS estimator for RSS prediction and obtained that for achieving good results the number of training samples should be limited (in our simulations we found the proper value is around ten, although the mobility model of the MS affects this value). The behaviour of the proposed approach was studied through extensive simulations using STEPS mobility model. The results show that the proposed handover algorithm achieves a lower OP and PPR and a higher throughout in comparison with the previous works.

In the current proposed algorithm, the sojourn time of MSs in each femtocell is not taken into account in the handover decision making. As a future work, we aim at improving our algorithm by considering sojourn times in addition to the RSS and SINR criteria.

doi: 10.1049/iet-com.2014.0230

7 References

1 Chandrasekhar, V., Andrews, J., Gatherer, A.: 'Femtocell networks: a survey', *IEEE Commun. Mag.*, 2008, **46**, pp. 59–67
2 Zhang, J., De la Roche, G.: 'Femtocells: technologies and deployment' (Wiley Online Library, 2010)
3 He, D., Chi, C., Chan, S., Chen, C., Bu, J., Yin, M.: 'A simple and robust vertical handoff algorithm for heterogeneous wireless mobile networks', *Wirel. Pers. Commun.*, 2011, **59**, pp. 361–373
4 Sung, N., Pham, N., Huynh, T., Hwang, W.: 'Predictive association control for frequent handover avoidance in femtocell networks', *IEEE Commun. Lett*., 2013, **17**, pp. 926–927
5 Li, H., Ci, S., Wang, Z.: 'Prediction handover trigger scheme for reducing handover latency in two-tier Femtocell networks'. 2012 IEEE Global Communications Conf. (GLOBECOM), 2012, pp. 5130–5135
6 Moon, J.-M., Cho, D.-H.: 'Efficient handoff algorithm for inbound mobility in hierarchical macro/femtocell networks', *IEEE Commun. Lett.*, 2009, **13**, pp. 755–757
7 Xu, P., Fang, X., He, R., Xiang, Z.: 'An efficient handoff algorithm based on received signal strength and wireless transmission loss in hierarchical cell networks', *Telecommun. Syst.*, **52**, 2013, pp. 1–9
8 Yidan, Z., Su, Z., Xiaorong, Z.: 'A new handover mechanism for femtocell-to-femtocell'. 2012 Int. Conf. on Wireless Communications & Signal Processing (WCSP), 2012, pp. 1–4
9 Dhahri, C., Ohtsuki, T.: 'Cell selection for open-access femtocell networks: learning in changing environment', *Phys. Commun.*, 2014, http://www.dx.doi.org/10.1016/j.phycom.2014.04.008, to be published
10 Sinclair, N., Harle, D., Glover, I.A., Atkinson, R.C.: 'A kernel methods approach to reducing handover occurrences within LTE'. 18th European Wireless Conf. European Wireless (EW) 2012, 2012, pp. 1–8
11 Zhou, H., Hu, D., Mao, S., Agrawal, P., Reddy, S.A.: 'Cell association and handover management in femtocell networks'. IEEE Wireless Communications and Networking Conf. (WCNC), 2013, 2013, pp. 661–666
12 Liu, C., Wei, J., Huang, S., Cao, Y.: 'A distance-based handover scheme for femtocell and macrocell overlaid networks'. Eighth Int. Conf. on Wireless Communications, Networking and Mobile Computing (WiCOM), 2012, 2012, pp. 1–4
13 Jeong, B., Shin, S., Jang, I., Sung, N.W., Yoon, H.: 'A smart handover decision algorithm using location prediction for hierarchical macro/femto-cell networks'. IEEE Vehicular Technology Conf. (VTC Fall), 2011, 2011, pp. 1–5
14 Sayed, A.H.: 'Adaptive filters' (Wiley.com, 2008)
15 Novlan, T., Andrews, J.G., Sohn, I., Ganti, R.K., Ghosh, A.: 'Comparison of fractional frequency reuse approaches in the OFDMA cellular downlink'. IEEE Global Telecommunications Conf. (GLOBECOM 2010), 2010, 2010, pp. 1–5
16 Lee, P., Lee, T., Jeong, J., Shin, J.: 'Interference management in LTE femtocell systems using fractional frequency reuse'. 12th Int. Conf. on Advanced Communication Technology (ICACT) 2010, 2010, pp. 1047–1051
17 Lee, J.Y., Bae, S.J., Kwon, Y.M., Chung, M.Y.: 'Interference analysis for femtocell deployment in OFDMA systems based on fractional frequency reuse', *IEEE Commun. Lett.*, 2011, **15**, pp. 425–427
18 '3GPP RP-110438, HetNet mobility improvements for LTE, Nokia Siemens Networks, Nokia Corporation, Alcatel- Lucent'
19 Chu, X., Wu, Y., Lopez-Perez, D., Tao, X.: 'On providing downlink services in collocated spectrum-sharing macro and femto networks', *IEEE Trans. Wirel. Commun.*, 2011, **10**, pp. 4306–4315
20 Gudmundson, M.: 'Correlation model for shadow fading in mobile radio systems', *Electron. Lett.*, 1991, **27**, pp. 2145–2146
21 Coifman, R.R., Wickerhauser, M.V.: 'Entropy-based algorithms for best basis selection', *IEEE Trans. Inf. Theory*, 1992, **38**, pp. 713–718
22 Schafhuber, D., Matz, G.: 'MMSE and adaptive prediction of time-varying channels for OFDM systems', *IEEE Trans. Wirel. Commun.*, 2005, **4**, pp. 593–602
23 Andreopoulos, Y., van der Schaar, M.: 'Adaptive linear prediction for resource estimation of video decoding', *IEEE Trans. Circuits Syst. Video Technol.*, 2007, **17**, pp. 751–764
24 Gibson, J.D.: 'Adaptive prediction in speech differential encoding systems', *Proc. IEEE*, 1980, **68**, pp. 488–525
25 Fout, N., Ma, K.-L.: 'An adaptive prediction-based approach to lossless compression of floating-point volume data', *IEEE Trans. Vis. Comput. Graph.*, 2012, **18**, pp. 2295–2304
26 Li, Y., Sayood, K.: 'Lossless video sequence compression using adaptive prediction', *IEEE Trans. Image Process.*, 2007, **16**, pp. 997–1007
27 Itoh, K.I., Watanabe, S., Shih, J.S., Sato, T.: 'Performance of handoff algorithm based on distance and RSSI measurements', *IEEE Trans. Veh. Technol.*, 2002, **51**, pp. 1460–1468
28 Lim, J.S., Oppenheim, A.V.: 'Advanced topics in signal processing' (Prentice-Hall, Inc., 1987)
29 Nguyen, A.D., Sénac, P., Ramiro, V., Diaz, M.: 'STEPS – an approach for human mobility modeling', NETWORKING 2011: (Springer, 2011, edn.), pp. 254–265
30 Liu, Z., Wang, J., Xia, Y., Yang, H.: 'Robust optimisation of power control for femtocell networks', *IET Signal Process.*, 2013, **7**, pp. 360–367
31 Bălan, I.M., Sas, B., Jansen, T., Moerman, I., Spaey, K., Demeester, P.: 'An enhanced weighted performance-based handover parameter optimization algorithm for LTE networks', *EURASIP J. Wirel. Commun. Netw.*, 2011, **2011**, pp. 1–11